

Investigations of the charge transport properties in $(\text{LaMn})_{0.956}\text{O}_3$ at low temperatures

This article has been downloaded from IOPscience. Please scroll down to see the full text article.

2006 J. Phys.: Condens. Matter 18 6691

(<http://iopscience.iop.org/0953-8984/18/29/010>)

View [the table of contents for this issue](#), or go to the [journal homepage](#) for more

Download details:

IP Address: 129.252.86.83

The article was downloaded on 28/05/2010 at 12:22

Please note that [terms and conditions apply](#).

Investigations of the charge transport properties in $(\text{LaMn})_{0.956}\text{O}_3$ at low temperatures

Woo-Hwan Jung

Division of Electronics, HoWon University, 727, Wolha-Ri, Impi, Kunsan Chun Buk, 573-930, Korea

E-mail: phdjung@sunny.howon.ac.kr

Received 12 April 2006, in final form 8 June 2006

Published 30 June 2006

Online at stacks.iop.org/JPhysCM/18/6691

Abstract

The magnetization, dc conductivity, and dielectric relaxation of cation-deficient manganese perovskite $(\text{LaMn})_{0.956}\text{O}_3$ have been investigated. $(\text{LaMn})_{0.956}\text{O}_3$ shows a ferromagnetic transition around 166 K and a thermally activated dielectric loss peak is observed in the ferromagnetic phase. The transport is thermally activated with a change in slope at the ferromagnetic transition. The temperature dependency of the dc conductivity and dielectric relaxation processes provide evidence of hopping conduction below T_C . The results have been discussed in terms of a hopping process of polarons localized by electron–lattice interaction in tandem with electron–magnon interaction.

1. Introduction

The colossal magnetoresistance (CMR) of doped manganese perovskite has attracted great attention for scientific studies and technological applications. The cubic (or pseudocubic) perovskite $\text{La}_{1-x}\text{A}_x\text{MnO}_3$ (A: Sr, Ca, etc) with a three-dimensional Mn–O network (isotropic MnO_6 octahedra) is known to become a conducting ferromagnet at hole doping concentrations of $x > 0.2$, and exhibit CMR effects [1–5]. Double exchange of $\text{Mn}^{3+}(t_{2g}^3 e_g^1) - \text{O}^{2-} - \text{Mn}^{4+}(t_{2g}^3)$ was proposed by Zener [6] to explain the simultaneous ferromagnetic and metallic state, and recently, in addition to double exchange interactions, strong electron–lattice coupling has been proposed as a mechanism to explain the CMR [7, 8].

It is interesting to note that ferromagnetism could be induced by simply creating cation vacancies at the La site even in the absence of any divalent ion substitution [9–15]. $\text{LaMnO}_{3+\delta}$ is the only compound of the LaMO_3 ($M = 3d$ transition metal ions) series that shows noteworthy oxygen excess. The oxygen excess δ , which cannot be accommodated interstitially in the lattice, results in equal amounts of La and Mn vacancies, $2 \times 100\delta$ of the corresponding percentage of Mn^{4+} . This series has been the subject of various crystallographic and magnetic studies [16]. Ritter *et al* [17] and Subias *et al* [18] found a continuous evolution from the highly distorted orthorhombic structure in LaMnO_3 towards a rhombohedral structure in

a $\delta = 0.15$ sample as δ increases. This structural change is accompanied by enhanced ferromagnetic interaction. Nevertheless, the $\text{LaMnO}_{3.15}$ compound, with the largest amount of La and Mn vacancies (4.8%), becomes a magnetically inhomogeneous compound without long-range ferromagnetism, showing instead a spin-glass-like behaviour [17, 18]. On the other hand, electrical resistivity measurements indicate an insulating state for any δ value at low temperatures. Such electrical and magnetic behaviour is interpreted in terms of the competition of La vacancies, which enhances the $\text{Mn}^{3+}/\text{Mn}^{4+}$ ratio, and Mn vacancies which induce disorder in the Mn sublattice, weakening the double exchange interaction. However, there is no general agreement and remarkably little is known about the transport mechanism in this kind of compound.

As mentioned above, the ferromagnetism could be induced by simply creating cation vacancies at the La site even in the absence of any divalent ion substitution, although the electronic properties of these kinds of materials remain insulating. The origin of this unexpected behaviour may give useful clues to the fundamental mechanism of the metal–insulator transition in the perovskite structure. Thus, the nature of the charge carrier responsible for conduction in the ferromagnetic phase of $(\text{LaMn})_{1-\lambda}\text{O}_3$ is expected to differ considerably from that of divalent ion doped LaMnO_3 . The aim of this work is to investigate the dc magnetic, conductivity, and dielectric relaxation properties in order to understand the origin of the charge carriers responsible for conduction in the ferromagnetic phase of cation-deficient $(\text{LaMn})_{1-\lambda}\text{O}_3$. As described in the literature, for materials in which hopping conduction dominates the electrical transport, dielectric measurements provide important information because the hopping process has a high probability of involving dielectric relaxation [19–22]. In this study, we have measured the complex dielectric properties of cation-deficient $(\text{LaMn})_{1-\lambda}\text{O}_3$ as a function of frequency (20 Hz–1 MHz) and temperature (77–300 K). We also measured the dc conductivity and magnetization.

2. Experiment

A polycrystalline sample was prepared by solid-state reaction of adequate quantities of La_2O_3 and MnO_2 (4 N grade). The La_2O_3 was heated to 1173 K in air for about 12 h prior to weighing. The desired mixture of preheated La_2O_3 and MnO_2 was heated 1173 K for 24 h. It was then ground, pelletized, and reheated to 1273 K for 24 h. This was repeated once again and the final heating was at 1373 K in pure oxygen gas for a period of 48 h. The oxygen content was analysed using a standard redox titration with a KMnO_4 solution. δ was found to be 0.14.

The sample was characterized by x-ray diffraction. The x-ray diffraction profiles were indexed with a rhombohedral unit cell ($R\bar{3}c$). Power diffraction was taken for $60^\circ < 2\theta < 104^\circ$ with 0.01° steps, scanning for the precise lattice parameter measurement. Silicon powder (5N) was mixed in as an internal standard. From the least-squares fitting method, we obtained the lattice parameter $a_R = 5.467 \text{ \AA}$ and rhombohedral angle (α) = 60.57° . The density of the sintered sample was about 85% of the theoretical values, which was calculated using the lattice constants from x-ray measurement. It has long been known that LaMnO_3 can exhibit a range of stoichiometry. The formula was given as $\text{LaMnO}_{3+\delta}$ in the early literature, but it is better written as $(\text{LaMn})_{1-\gamma}\text{O}_3$ [12, 23] reflecting the presence of cation vacancies rather than oxygen excess. If the number of La and Mn vacancies is assumed to be equal, then δ and γ are related by $\gamma = \delta/(3 + \delta)$. Based upon this reasoning, the effective chemical formula of the present compound must be represented as $(\text{LaMn})_{0.956}\text{O}_3$. The cation concentration ratio estimated by electron probe microanalyser nearly agrees with the nominal value.

The dc magnetization was measured using a SQUID magnetometer (Quantum Design MPMS). The magnetization–temperature (M – T) curve was measured under the ZFC (zero-

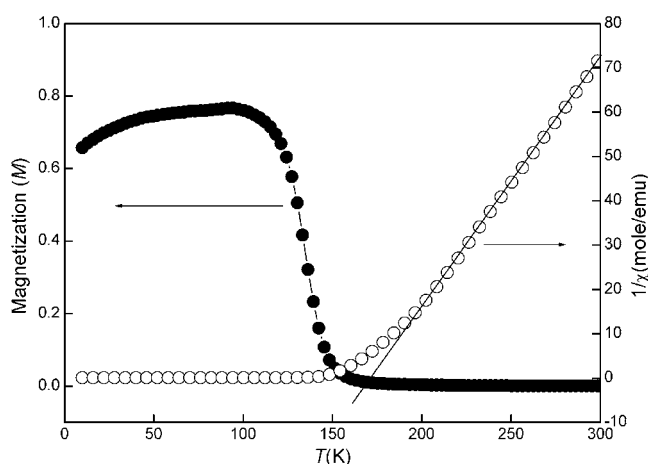


Figure 1. The temperature dependence of the reciprocal susceptibility measured with a magnetic field of 100 Oe (open circles). The straight line represents the Curie–Weiss law. The temperature dependence of the magnetization measured with a magnetic field of 100 Oe (solid circles).

field-cooled) condition, which consisted of heating the sample to 300 K after zero-field cooling to 4.2 K, applying a field of 100 Oe. A Keithley 619 Resistance Bridge, an Advantest TR 6871 digital multi-meter, and an Advantest R6161 power supply were used for the conductivity measurement using the four-probe method. Capacitance and impedance were obtained as function of temperature up to 300 K by the four-terminal pair ac impedance measurement method using an HP 4194A impedance/gain phase analyser. Flat surfaces of the specimen were coated with an In–Ga alloy in 7:3 ratio by a rubbing technique, to act as an electrode. Evaporated gold was also used for the electrode, but no significant difference was found in the experimental results.

3. Results and discussion

Figure 1 demonstrates the temperature dependence of the reciprocal molar magnetic susceptibilities ($1/\chi$) for $(\text{LaMn})_{0.956}\text{O}_3$. The relation of $1/\chi$ to T (open circles) for the sample contains a linear portion above 220 K, which is indicative of the Curie–Weiss law with the formula $\chi = C/(T - \Theta)$, where C is the Curie constant and Θ is the Weiss temperature. The effective magnetic moment ($\mu_{\text{eff}} = \sqrt{8C}\mu_{\text{B}}$) is estimated to be $5.64\mu_{\text{B}}$.

The magnetization measured after ZFC under 100 Oe is also plotted (solid circles) as a function of temperature in figure 1. The ferromagnetic Curie temperature T_{C} is determined by the conventional M^2 – T method. The magnetic transition temperature is determined to be 168 K. The steep rise in the magnetization with decrease in temperature around T_{C} indicates a phase transition from a paramagnetic to a ferromagnetic state.

The temperature dependence of the electrical conductivity (σT) is shown in figure 2. The conductivity of the present material showed a semiconducting temperature dependence and became too low to measure at low temperatures, i.e., $(\text{LaMn})_{0.956}\text{O}_3$ is a ferromagnetic insulator.

Figure 3 plots the dielectric loss tangent ($\tan \delta$) and electric modulus (imaginary part, M'') as a function of applied frequency at several temperatures. It should be noted that dielectric relaxation occurs in the ferromagnetic spin regime, whereas in the low temperature region

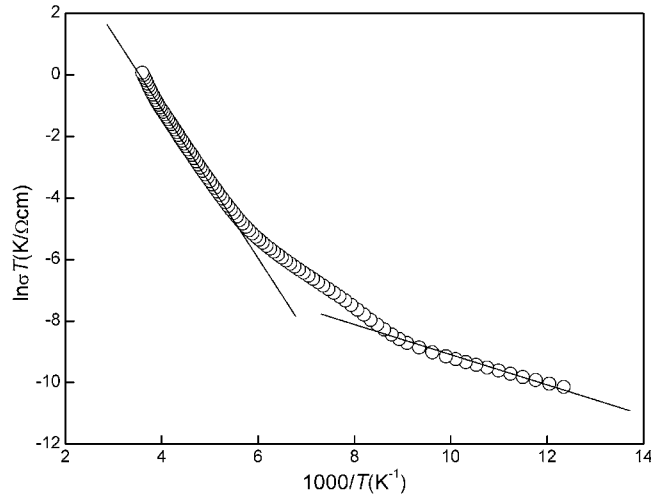


Figure 2. Arrhenius relation between σT and $1/T$ for $(\text{LaMn})_{0.956}\text{MnO}_3$. $(\text{LaMn})_{0.956}\text{MnO}_3$ contains two thermally activated processes represented by the solid straight lines.

a thermally activated process governs conduction. Above 120 K, no resonance peak was recognized in the frequency range employed in the present work. This fact implies that the resonance peak disappears at high temperatures or the dielectric relaxation process requires a frequency much higher than the 1 MHz maximum frequency used in the present work (if it exists above 120 K). The distortions introduced by the excess oxygen and associated vacancies are sufficient to produce more than one off-centre equilibrium position for the Mn^{4+} ions. The observed relaxation is associated with thermally activated motion between these equivalent potential minima. The temperature and frequency dependence of the dielectric properties in this region can be described by a Debye relaxation mechanism [24]. The dielectric loss tangent and dielectric modulus are [20, 21]

$$\tan \delta = \frac{\varepsilon''}{\varepsilon'} = \frac{(\varepsilon_0 - \varepsilon_\infty)\omega\tau_0}{\varepsilon_0^2 + \varepsilon_\infty^2(\omega\tau_0)^2} \quad (1)$$

$$M'' = \frac{(\varepsilon_0 - \varepsilon_\infty)\omega\tau_0}{\varepsilon_0^2 + \varepsilon_\infty^2(\omega\tau_0)^2} \quad (2)$$

where $M^* = M' + jM'' = 1/(\varepsilon' - \varepsilon'')$ and $\tau_0 = (\varepsilon_0 + 2)\tau/(\varepsilon_\infty + 2)$. At temperature T , the loss tangent ($\tan \delta$) and electric modulus (M'') have maxima at the resonance frequencies, $f_{\tan \delta}$ and $f_{M''}$, i.e., $f_{\tan \delta} = \sqrt{\varepsilon_0/\varepsilon_\infty}/2\pi\tau$ and $f_{M''} = (\varepsilon_0/\varepsilon_\infty)/2\pi\tau$, where ε_0 and ε_∞ are the static and high frequency dielectric constants, and τ is the relaxation time, which is proportional to $\exp(-Q/k_B T)$, Q being the activation energy for dielectric relaxation. These relations yield the dielectric resonance condition at temperature T as $(f_{\tan \delta})^2/f_{M''} \propto \exp(-Q/k_B T)$. Figure 4 displays Arrhenius plots of $(f_{\tan \delta})^2/f_{M''}$ and $1/T$. The least-mean-square analysis yields $Q = 0.04$ eV.

Part of the dielectric strength is due to a thermally activated process, which is related to the dipolar unit [22]. In this case, there is another dielectric relaxation $T(\tan \delta)_{\max}^2/M''_{\max} \propto \exp(-W_0/2k_B T)$, where $(\tan \delta)_{\max}$ and M''_{\max} are maxima of the loss tangent and electric modulus at T , respectively. Mobile carriers are created by releasing holes trapped at imperfections by W_0 , which is the potential difference between a free carrier and a carrier bound to a trap [25, 26]. For $(\text{LaMn})_{0.956}\text{O}_3$, Mn vacancies must play a somewhat important

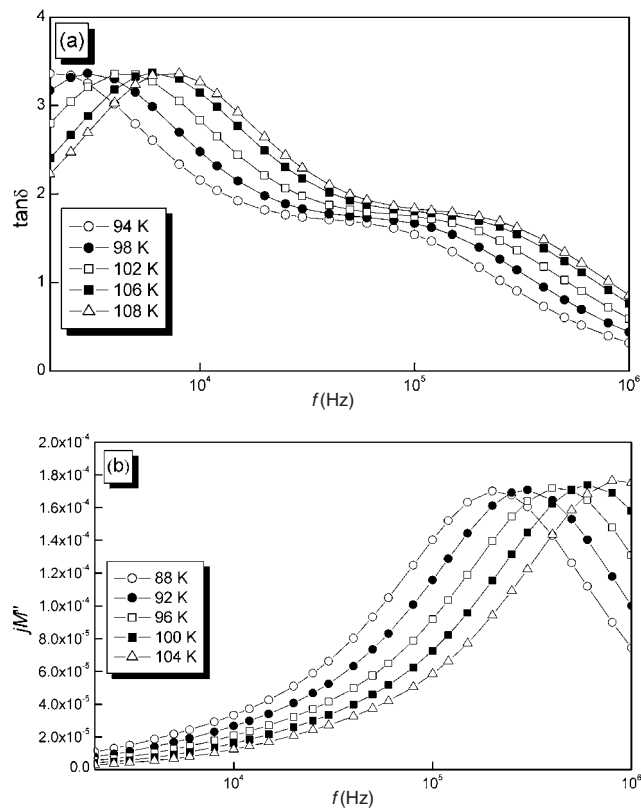


Figure 3. Frequency dependence of the dielectric loss tangent ($\tan \delta$) and electrical modulus (imaginary part, M'') at several temperatures for specimens of $(\text{LaMn})_{0.956}\text{MnO}_3$; (a) $\tan \delta$ and (b) M'' .

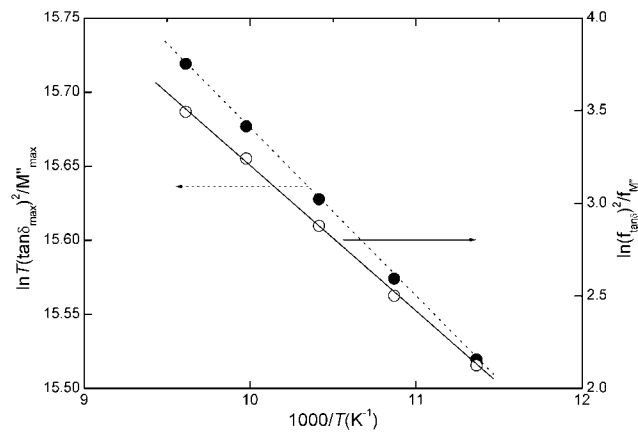


Figure 4. The Arrhenius relation between $(f_{\tan \delta})^2 / f_{M''}$ (solid line), $1/T$ and $T (\tan \delta)_{\max}^2 / M''_{\max}$ (dotted line).

role in the formation of traps. The Arrhenius relation of $T (\tan \delta)_{\max}^2 / M''_{\max}$ and $1/T$ shown in figure 4 yields $W_0/2 = 0.043$ eV. These results suggest that the spectral intensity of the loss

tangent observed in $(\text{LaMn})_{0.956}\text{O}_3$ is thermally activated like the dielectric relaxation occurring in various other materials, in which the process of hopping of non-adiabatic and/or adiabatic small polarons dominates the electrical transport [19–22, 25, 26].

The balance between stoichiometry, structure, and the resistivity behaviour of $\text{La}_{0.9}\text{MnO}_{3-\delta}$ samples has been investigated by Maignan *et al* [27], who found a metal–insulator transition in all samples with a monoclinic structure, but semiconducting behaviour in samples with an orthorhombic structure. This is attributed to variations in the oxygen content affecting the Mn^{4+} content, as the semiconducting sample has a higher value of δ . A metal–insulator transition was also observed by Mahendiran *et al* [28] in $(\text{LaMn})_{1-x}\text{O}_3$ samples with $x = 0.04$ and 0.055 , although a sample with $x = 0.02$ showed semiconducting behaviour throughout the temperature range studied. This was also attributed to the doping effect whereby above a threshold concentration of Mn^{4+} , a metal–insulator transition is observed. Töpfer *et al* [29] also studied samples of $\text{LaMnO}_{3+\delta}$ with $0.08 \leq \delta \leq 0.16$. For low values of δ , semiconducting behaviour is observed, although as δ is increased some metallic behaviour is observed at low temperatures (<75 K) which disappears with the evolution of variable-range hopping at even lower temperatures (<40 K). They suggested that a higher vacancy concentration would result in samples showing metal–insulator transitions, as the number of charge carriers was increased in order to overcome the competing effect of localization due to vacancies.

The value of $\gamma = 0.044$ in this study corresponds to $\delta = 0.14$, which is very similar in composition to a sample measured by Mahendiran *et al* [28] and Töpfer *et al* [29] which showed a complete metal–insulator transition. Although the $(\text{LaMn})_{0.956}\text{O}_3$ compound shows a ferromagnetic contribution at low temperatures (see figure 1), the $(\text{LaMn})_{0.956}\text{O}_3$ is found to be insulating throughout the range of temperatures. According to a Mn K-edge XAS study by Subias *et al* [18], the insulating temperature dependence of resistivity below T_C in heavily cation-deficient LaMnO_3 compounds must be related to the presence of Mn vacancies. The Mn vacancies give rise to a randomization of the magnetic interaction and this inhomogeneous magnetic state must be related to the local structural distortion of the low temperature phase, as has been found in related compounds. Ranno *et al* [23] suggest that the potential fluctuations due to the missing Mn ions can favour the Anderson localization of current carriers, with localized wavepackets large enough for the e_g electrons to extend over several sites, providing short-range ferromagnetic interaction.

The missing Mn ion is strongly correlated to the reduction of the mobility of charge carriers. The presence of a large Mn vacancy concentration may cause competition between the ferromagnetic and antiferromagnetic interactions. In addition, the presence of Mn vacancies in $(\text{LaMn})_{0.956}\text{O}_3$ may be large enough to induce local lattice distortion and consequent polaron formation in the low temperature phase, an idea proposed by Ranno *et al* [23] and Subias [18].

If conduction in the high ($T > T_C$) and low ($T < T_C$) temperature phases proceeds via hopping of polarons, we obtain for the electrical conductivity [19–21, 30]

$$\sigma T^\alpha = \sigma_0 \exp(-W_H/k_B T) \quad (3)$$

with $\alpha = 1$ according to the Emin–Holstein theory of adiabatic small polaron hopping [30], where W_H is the small polaron hopping energy. In figure 3, there are two activated process in conduction, one that is above T_C and one below T_C , i.e., the linear portion above T_C with an activation energy of 0.16 eV and one below T_C with an activation energy of 0.086 eV. In the low ($T < T_C$) and high ($T > T_C$) temperature regions, the linear relation in the Arrhenius plot of σT and $1/T$ surely favours the polaronic theory. When the process of hopping of small polarons dominates conduction, Q and W_H are represented as $W_H \cong Q + W_0/2$ [19–21, 25, 26, 30]. The activation energy must be the sum of the hopping energy

W_{H} and the disorder energy, because the random distribution of Mn^{3+} and Mn^{4+} ions results in a disorder of potentials on Mn^{3+} and Mn^{4+} ions.

This discussion starts from the low temperature conduction process in the ferromagnetic insulator below T_{C} . The magnetic properties of $(\text{LaMn})_{0.956}\text{O}_3$ indicate that the charge carrier involves a component from a spin polaron. In ferromagnetic insulators, there is a high possibility that carriers are spin polarons. Kasuya and Yanase [31] considered the behaviour of pure spin polarons, defined as charge carriers localized at impurity centres by polarization clouds, with a transport mechanism of thermal hopping between sites. In this theory, the activation energy for electrical conduction is the energy of the trapping of carriers by impurity centres, i.e., $W_{\text{H}} = W_0$. For $(\text{LaMn})_{0.956}\text{O}_3$, however, the present study distinguishes the hopping energy from the trapping energy.

Emin *et al* [32, 33] considered the nature of lattice polarons in ferromagnetic insulators. In this model, spin polarons are carriers self-localized by the intra-atomic exchange due to the electron–magnon interaction in tandem with the short-range component of the electron–lattice interaction. Thus, a hopping process of spin polarons could be observed experimentally in ferromagnets, but with a rather low activation energy. In fact, the spin polaron theory is indicative of an extremely low activation energy for a hopping process of spin polarons. In the case of the existence of spin polarons there is a magnetic exchange contribution to the activation energy. In the low temperature region (ferromagnetic phase), dielectric relaxation due to the hopping process is observed for $(\text{LaMn})_{0.956}\text{O}_3$. This must be due to the ferromagnetic component as described before. Thus, electron–magnon interaction is expected in the low temperature region. According to Kusters *et al* [34], the electron–magnon interaction drives the carriers towards localization, like the electron–lattice interaction, and becomes important particularly at temperatures close to the onset of ferromagnetism. By analogy with their result, the present system is expected to experience a similar situation, namely both lattice and magnetic characteristics govern the nature of the charge carriers. The electrical transport in $(\text{LaMn})_{0.956}\text{O}_3$ below T_{C} is then likely to be rather close to that in the conduction picture constructed by Emin *et al* [32, 33].

Equation (3) describes the motion of a polaron in an undistorted background trapped in its own potential [35]. Here the localized carrier distorts the surrounding lattice and magnetically polarizes the manganese atoms in the neighbourhood, thereby gaining exchange energy and forming a bound spin polaron. This concept was introduced by de Gennes [36]. Even well above T_{C} these spin polarons exist, as shown experimentally by de Teresa *et al* [37] with small-angle neutron scattering measurements and theory by Gehring and Coombes [38]. Thus, the theoretical formulae representing the dc conduction above T_{C} cannot change. The Arrhenius relation of σT and $1/T$ above T_{C} favours polaron hopping conduction, but the energy required for conduction is higher than that below T_{C} . We think that in the low temperature region ($T < T_{\text{C}}$) localization of charge carriers results from chemistry (random Mn vacancies), and spin disorder. With the increase of temperature, the effect of spin disorder becomes more pronounced, and thus the charge carriers in the paramagnetic phase are localized more deeply; this must be one of the main reasons for the result of high hopping energy above T_{C} .

4. Conclusion

We have confirmed the paramagnetic–ferromagnetic transition in a La- and Mn-deficient compound $(\text{LaMn})_{0.956}\text{O}_3$ without any divalent substitution at the La site. The transport is thermally activated with a change in slope at the ferromagnetic transition. This fact implies that the variation of spin disorder with increasing temperature provides a magnetic contribution to the activation energy of polarons for hopping. A dielectric relaxation appears in the loss

tangent and electric modulus below T_C . The activation energy required for relaxation is nearly equal to that for conduction below T_C . The results have been discussed in terms of a process of hopping polarons localized by the electron–lattice interaction in tandem with electron–magnon interaction.

Acknowledgment

This project was supported by HoWon University.

References

- [1] Jin S, Tiefel T H, McCormack M, Fastnacht R A, Ramesh R and Chen L H 1994 *Science* **264** 413
- [2] Schiffer P, Ramirez A P, Bao W and Cheong S W 1995 *Phys. Rev. Lett.* **75** 3336
- [3] Hwang H Y, Cheong S W, Radaelli P G, Marezio M and Batlogg B 1995 *Phys. Rev. Lett.* **75** 914
- [4] Park J H, Chen C T, Cheong S W, Bao W, Meigs G, Chakraborty V and Idzerda Y U 1996 *Phys. Rev. Lett.* **72** 4215
- [5] Radaelli P G, Marezio M, Hwang H Y, Cheong S W and Batlogg B P 1995 *Phys. Rev. Lett.* **75** 4488
- [6] Zener C 1951 *Phys. Rev.* **82** 403
- [7] Röder H, Zang J and Bishop R 1996 *Phys. Rev. Lett.* **76** 1356
- [8] Mills A J, Shraiman B I and Müller R 1996 *Phys. Rev. Lett.* **77** 175
- [9] Manoharan S, Kumar D, Hegde M S, Satyalakshmi K N, Prasad V and Subramanyam S V 1995 *J. Solid State Chem.* **117** 420
- [10] van Roosmalen J A M, van Vlaanderen P, Cordfunke E H P, Ijdo W L and Ijdo D J W 1995 *J. Solid State Chem.* **114** 516
- [11] Hauback B C, Fjellvåg H and Sakai N 1996 *J. Solid State Chem.* **124** 43
- [12] Dörr K, Müller K H, Vlahov E S, Chakalov R A, Chakalov R I, Nenkov K A, Handstein A, Holzapfel B and Schultz L 1998 *J. Appl. Phys.* **83** 7079
- [13] Suryanaryanan R, Berthon J, Zelenay I, Martinez B, Obrador X, Uma S and Gmelin E J 1998 *Appl. Phys.* **83** 5264
- [14] de Silva P S I P N, Richards F M, Cohen L F, Alonso J A, Martínez-Lope M J, Casais M T, Thomas K A and MacManus-Driscoll J L 1998 *J. Appl. Phys.* **83** 394
- [15] Zao Y G, Rajeswari M, Srivastava R C, Biswas A, Ogale S B, Kang D J, Prellier W, Chen Z, Greene R L and Venkatesan T J 1999 *Appl. Phys.* **86** 6327
- [16] Töfeld B C and Scott W R 1974 *J. Solid State Chem.* **10** 183
- [17] Ritter C, Ibarra M R, de Teresa J M, Algaravel P A, Marquina C, Blasco J, García J, Oseroff S and Cheong S W 1997 *Phys. Rev. B* **56** 8092
- [18] Subías G, García J, Blasco J and Proietti M G 1998 *Phys. Rev. B* **58** 9287
- [19] Jung W H and Iguchi E 1996 *Phil. Mag. B* **73** 873
- [20] Iguchi E, Ueda K and Jung W H 1996 *Phys. Rev. B* **54** 17431
- [21] Jung W H, Nakatsugawa H and Iguchi E 1997 *J. Solid State Chem.* **133** 466
- [22] Chern G, Hsich W K, Tai M F and Hsung K S 1998 *Phys. Rev. B* **58** 1252
- [23] Ranno L, Viret M, Mari A, Thomas R M and Coey J M D 1996 *J. Phys.: Condens. Matter* **8** L33
- [24] Fröhlich H 1958 *Theory of Dielectrics* (Oxford: Clarendon) p 70
- [25] Jung W H and Iguchi E 1998 *J. Phys. D: Appl. Phys.* **31** 794
- [26] Iguchi E, Nakatsugawa H and Futakuchi K 1998 *J. Solid State Chem.* **139** 176
- [27] Maignan M, Simon C, Caignaert V and Raveau B 1996 *J. Appl. Phys.* **79** 7891
- [28] Mahendiran R, Tiway S K, Raychaudhuri A K, Ramakrishnan T V, Mahesh R, Rangavittal N and Tao C N R 1996 *Phys. Rev. B* **53** 3348
- [29] Töpfer J, Doumerc J and Grenier J 1996 *J. Mater. Chem.* **6** 1511
- [30] Emin D and Holstein T 1969 *Ann. Phys.* **53** 439
- [31] Kasuya T and Yanase Y 1968 *Rev. Mod. Phys.* **40** 684
- [32] Emin D, Hilley M S and Liu N H 1986 *Phys. Rev. B* **33** 2933
- [33] Emin D, Hilley M S and Liu N H 1987 *Phys. Rev. B* **35** 641
- [34] Kuster R M, Singleton J, Keen D A, McGreevy R and Hayes W 1989 *Physica B* **155** 362
- [35] Jakob G, Westerburg W, Martin F and Adrian H 1998 *Phys. Rev. B* **58** 14966
- [36] de Gennes 1960 *Phys. Rev.* **118** 141
- [37] Teresa M De, Ibarra M R, Algaravel P A, Ritter C, Marquina C, Blasco J, García J, del Moral A and Arnold Z 1997 *Nature* **386** 256
- [38] Gehring G A and Coombes D 1998 *J. Magn. Magn. Mater.* **177–181** 873